New Extended Defects in the Superconductive "123" Oxycarbonitrate $YCaBa_4Cu_5(NO_3)_x(CO_3)_{1-x}O_{11}$: HREM Study

M. Hervieu,* C. Michel, and B. Raveau

Laboratoire CRISMAT associé au CNRS, ISMRA/Université de Caen, Bd du Maréchal Juin, 14050 CAEN Cedex, France

Received March 29, 1993. Revised Manuscript Received May 18, 1993

A HREM study of the 72 K superconductor $YCaBa_4Cu_5(NO_3)_x(CO_3)_{1-x}O_{11}$ has been performed. One observes, for many crystals, a very regular contrast characteristic of the "$2a_{123} \times b_{123} \times 2c_{123}$" superstructure corresponding to an ordered stacking of the rows of CuO_5 pyramids and of CO_3 (NO_3) groups along $\vec{a}$, alternately. Contrary to $YBa_2Cu_3O_7$, this compound does not exhibit any microtwinning in agreement with the pseudotetragonal character of its subcell. One observes three kinds of extended defects: (i) Intergrowths of other n members of the series $(Y_{1-x}Ca_x)_nBa_{2n}Cu_{3n-1}(NO_3)_x(CO_3)_{1-x}O_{7n-3}$, involving different local superstructures with $a = 3a_{123}$, $4a_{123}$, and $6a_{123}$; this suggests strongly the possibility to synthesize the members n = 3, 4, and 6. (ii) 90° oriented domains similar to those previously observed for "123" type oxycarbonates, whose junctions have been interpreted. (ii) Intergrowths of the "123" oxycarbonitrate and the $Sr_2CuO_2CO_3$-type structure. These defects are of capital important since they are the signature of the possible existence of a new series of oxycarbonates or nitrates, $(Y_{1-x}Ca_x)_2A_2Cu_4O_9(A_2CuO_2MO_3)_n$ for A = Ba, Sr; M = C, N with an original structure and which might be superconductive.

Introduction

The introduction of nitrate groups in the "123" matrix, recently demonstrated,[1] leads to a new superconductor, $YCaBa_4Cu_5(NO_3)_{0.3}(CO_3)_{0.7}O_{11}$, with a T_c(onset) of 82 K. This oxycarbonitrate can be considered as the second member of a large family with the formulation $(Y_{1-x}Ca_x)_nA_{2n}Cu_{3n-1}(MO_3)O_{7n-3}$,[2] in which A = Ba, Sr and M = C, N, or B; several other members of this series, involving triangular carbonate groups have indeed been isolated.[3-10]

The high flexibility of this structure in which triangular CO_3 or NO_3 groups replace, partly and in a more or less ordered way, the CuO_4 square-planar groups suggests the possible existence of original extended defects. The study of the latters by high-resolution electron microscopy is primordial since they may influence the superconducting properties of these materials but also because this investigation may allow new superconductors with an original structure to be discovered. Moreover, the coexistence of

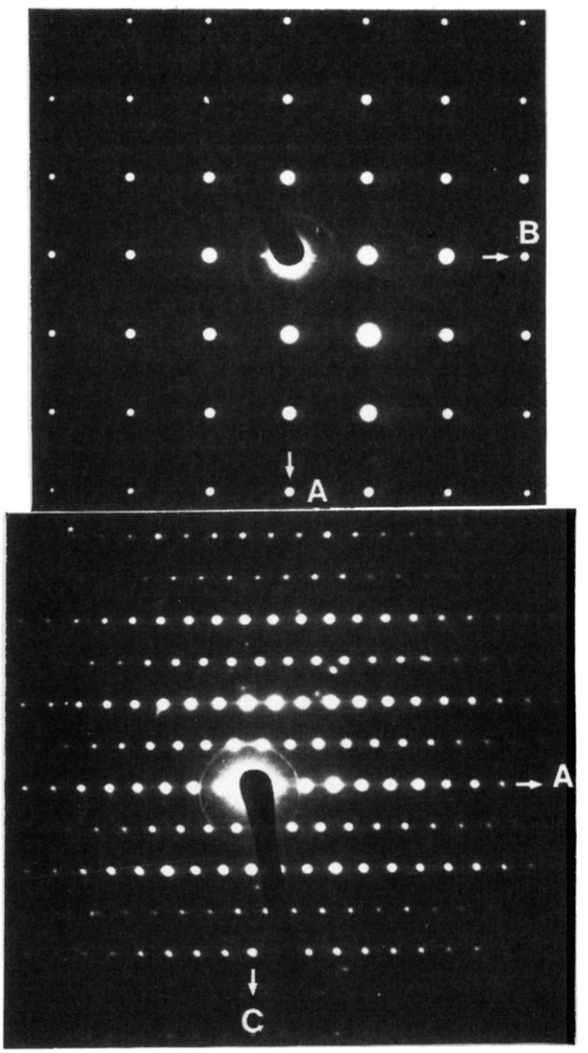

Figure 1. (a) [001] and (b) [010] electron diffraction patterns of $YCaBa_4Cu_5(NO_3)_{0.3}(CO_3)_{0.7}O_{11}$.

(1) Maignan, A.; Hervieu, M.; Michel, C.; Raveau, B. *Physica C* **1993,** *208,* 116.
(2) Raveau, B.; Huvé, M.; Maignan, A.; Hervieu, M.; Michel, C.; Domengès, B.; Martin, C. *Physica C,* in press.
(3) Domengès, B.; Hervieu, M.; Raveau, B. *Physica C,* in press.
(4) Miyazaki, H.; Yamane, H.; Ohnishi, N.; Kajitani, T.; Hiraga, K.; Morii, Y.; Funahashi, S.; Hirai, T. *Physica C* **1992,** *198,* 7.
(5) Miyazaki, Y.; Yamane, H.; Hirai, T. *Physica C* **1992,** *198,* 53.
(6) Zhu, W. J.; Ye, J. J.; Huang, Y. Z.; Zhao, Z. X. *Physica C* **1993,** *205,* 118.
(7) Akimitsu, J.; Ueharie, M.; Ogawa, M.; Nakata, H.; Tomimoto, T.; Miyazaki, Y.; Yamane, Y.; Hirai, T.; Kinoshita, K.; Matsui, Y. *Physica C* **1992,** *201,* 320.
(8) Miyazaki, Y.; Yamane, H.; Kobayashi, N.; Hirai, T.; Nakata, H.; Tomimoto, K.; Akimitsu, J. *Physica C* **1992,** *202,* 162.
(9) Hervieu, M.; Boullay, Ph.; Domengès, B.; Maignan, A.; Raveau, B. *J. Solid State Chem.,* in press.
(10) Domengès, B.; Boullay, Ph.; Hervieu, M.; Raveau, B. *J. Solid State Chem.,* submitted.
(11) Caignaert, V.; Hervieu, M.; Wang, J.; Desgardin, G.; Raveau, B.; Boterel, F.; Haussonne, J. M. *Physica C* **1990,** *170,* 139.
(12) Hervieu, M.; Domengès, B.; Provost, J.; Deslandes, F.; Raveau, B. *Ange. Chem.* **1988,** *27,* 440.
(13) Domengès, B.; Hervieu, M.; Michel, C.; Maignan, A.; Raveau, B. *Phys. Stat. Solidi A* **1988,** *107,* 73.

0897-4756/93/2805-1126$04.00/0

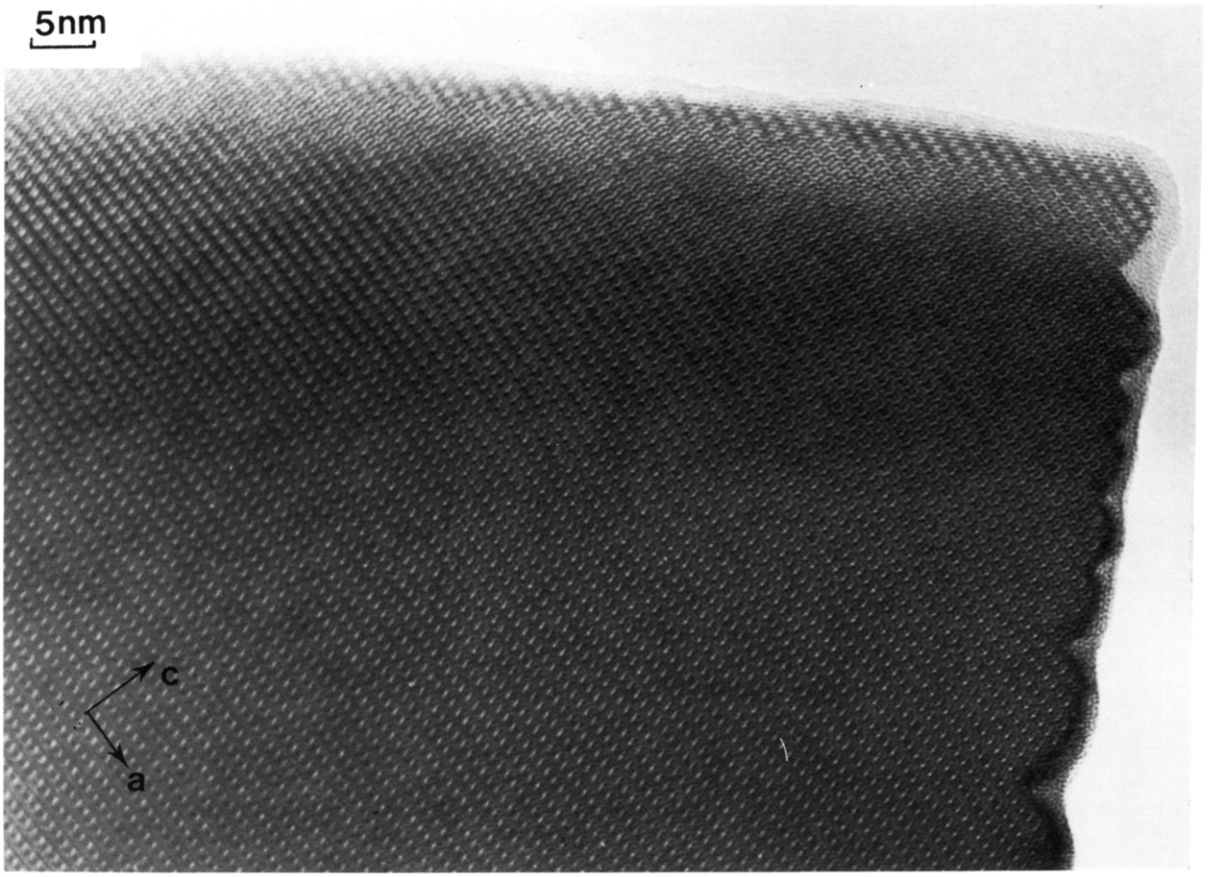

Figure 2. Overall [010] image: the periodicity $2 \times a_{123}$ and $2 \times c_{123}$ is well established throughout the crystal.

nitrate and carbonate groups in the same matrix is susceptible to induce specific defects with respect to carbonates. This paper deals with the HREM study of this new oxycarbonitrate. It shows the existence of novel defects with respect to carbonates, which must be considered as starting points for the generation of new oxycarbonates or nitrates with eventual superconducting properties.

Experimental Section

The synthesis of the phases was performed from a mixture of the oxides Y_2O_3, CaO, $BaCuO_2$, and CuO and of barium nitrate $Ba(NO_3)_2$ as previously described.[1] The intimate mixtures are pressed in the form of bars, placed in evacuated tube, and heated at 900 °C for 24–48 h; they are furnace cooled down to room temperature.

The EDX analysis was performed with a KEVEX analyzer mounted on the electron microscopes. The chemical analysis of carbon and nitrogen was performed by combustion in oxygen flow and coulometric titration (Service Central d'Analyse of CNRS). They lead to the formulation $YCaBa_4Cu_5(NO_3)_{0.33}(CO_3)_{0.66}O_{11}$.[1]

The electron diffraction (ED) study was performed with a JEOL 200CX electron microscope fitted with an eucentric goniometer (±60°). The high-resolution electron microscopy (HREM) is performed with a TOPCON 002B electron microscope operating at 200 kV (objective lens aberration constant of 0.4 mm). The samples are prepared from smooth crusching in *n*-butanol; the microcrystals are deposited on a holey carbon film supported by an aluminium grid.

Results and Discussion

The Regular Crystals. Reconstructions of the reciprocal space confirm that the superstructure $2a_{123} \times a_{123} \times 2c_{123}$ is established in numerous crystals; the superstructure reflections are strong as shown from the [010] ED pattern (Figure 1b). The conditions of reflection are hkl, $h + l = 2n$ leading to the $Bmmm$, $B222$, or $Bm2m$ as possible space groups (Figure 1a,b).

The most typical contrast of the HREM images consists of rows of small white dots, lined up along $\tilde{a}$ (Figure 2) with a periodicity of 7.7 Å corresponding to $a \approx 2a_{123}$; these rows are spaced of 11.4 Å (c_{123}) but the white dots are shifted of $\tilde{a}_{123}$ in one row with regard to the adjacent ones so that $c = 2c_{123}$. This contrast is typical of the structure of the 123-type oxycarbonate $Y_{1.2}Ca_{0.8}Ba_4Cu_5CO_3O_{11}$ (Figure 3b) which corresponds to the ordered substitution of one row of the square planar groups out of two in the 123 structure (Figure 3a).[9,10] The white dots are correlated to the rows of CO_3 or NO_3 groups at the level of Cu(1) in the intermediate layer of the 123 structure. Such images confirm that the substitution is ensured in an almost regular way throughout the crystals. For the HREM images, another focus value which allows to enhance the contrast at the level of the nitrate or carbonate groups is shown in Figure 4a; it consists of small crosses of white dots, centered by a gray dot and separated by black dots.

The recording of numerous images shows an even contrast on the crystal edges from one crystal to the other; this suggests that no difference can be made between nitrate and carbonate groups in agreement with the similar scattering factors of N and C and the identical geometry and size of the NO_3 and CO_3 groups. In these conditions, we have interpreted our contrast using the simulated images calculated for the oxycarbonate $(Y_{1-x}Ca_x)_2Ba_4Cu_5CO_3O_{11}$.[10] The characteristic contrasts are observed for focus values close to −10 (Figure 4), + 10 nm, and +

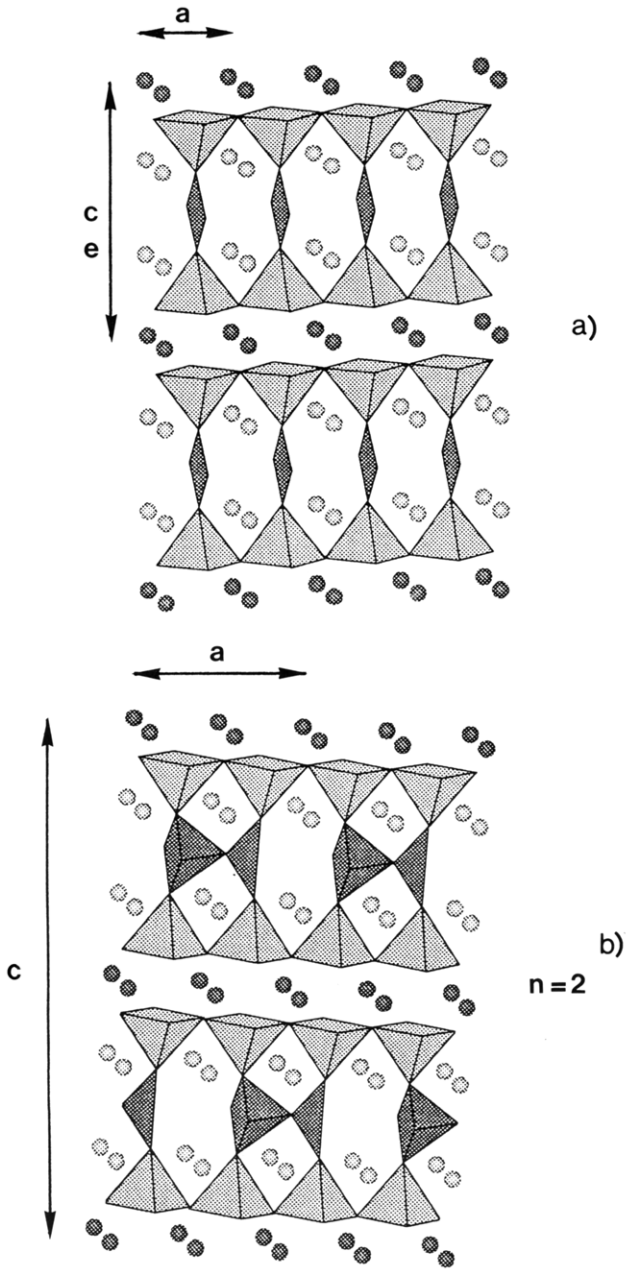

Figure 3. Idealized drawing of (a) the 123-type structure and (b) the $n = 2$ member of the oxycarbonate and/or oxycarbonitrate where a row of CuO_4 square groups is replaced by a row of NO_3 and/or CO_3 groups.

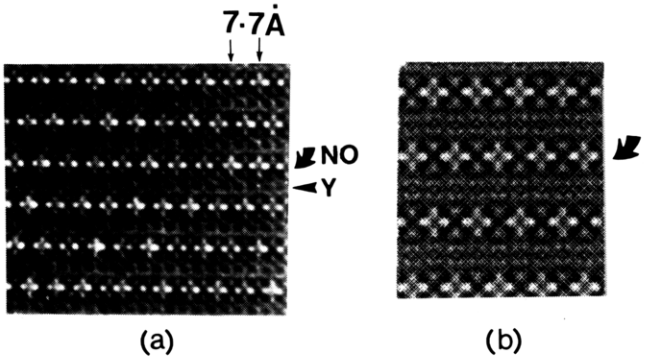

Figure 4. (a) Experimental and (b) enlarged calculated images for a focus value of −10 nm.

20 nm (Figure 2). In Figure 4, along the mixed row (curved arrow), the gray dots are correlated to N or C atoms, the black ones to copper, and the white dots of the crosses to

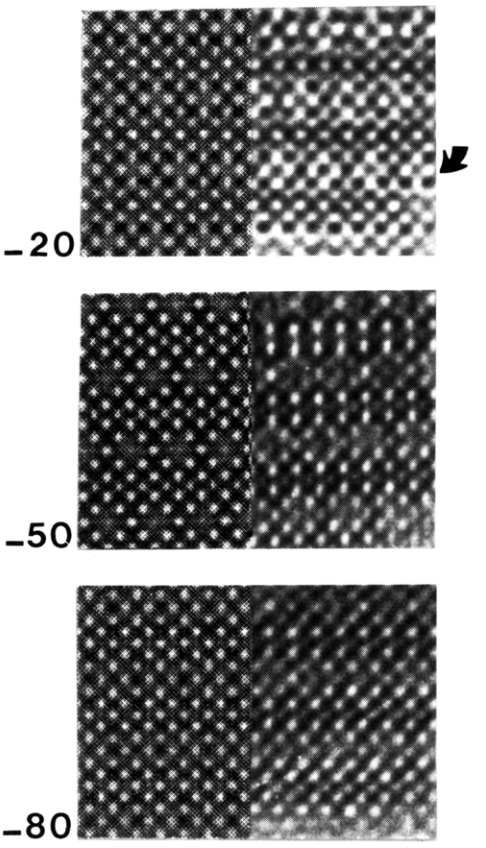

Figure 5. Comparison of the calculated and experimental images for Δf = −20, −50, and −80 nm.

oxygens and vacancies surrounding the (N, C) atoms (Figure 4b). In Figure 2, the white dots are correlated to N, C atoms positions. The calculated[10] and experimental images for some classical focus values are compared in Figure 5a–c. For −20 nm (Scherzer value) and −80 nm the cations positions appear as black dots, whereas for −50 nm they appear as bright dots, except the C and N atoms which present a very weak contrast. These images confirm the structural model and show that for some focus values the superperiodicity is scarcely visible; the interpretation of the structural phenomena needs then the recording of the through focus series.

Extended Defects. Besides the numerous grains which exhibit a highly regular contrast, one observes several kinds of extended defects which can be classified in three categories corresponding to the appearance of other n members in the matrix, to the existence of oriented domains and to the formation of intergrowths of the "123" oxycarbonitrates with the $Sr_2CuO_2CO_3$ type structure.[14-17]

(1) Intergrowth of Other n Members of the Series $(Y_{1-x}Ca_x)_nBa_{2n}Cu_{3n-1}MO_3O_{7n-3}$.

The regularity of the stacking of the rows of MO_3 groups (M = C, N) and CuO_5 pyramids is sometimes broken. This phenomenon corresponds to the local formation of other members of the series $(Y_{1-x}Ca_x)_nBa_{2n}Cu_{3n-1}MO_3O_{7n-3}$. Examples are shown in Figure 6. In Figure 6a, for a focus value close to 10 nm, we observe clearly the rows of white

(14) Deleted in proof.

(15) Chaillout, C.; Huang, Q.; Cava, R. J.; Chenavas, J.; Santoro, A.; Bordet, P.; Hodeau, J. L.; Kajewskii, J. J.; Levy, J. P.; Marezio, M.; Peck Jr., W. F. *Physica C* **1992**, *195*, 335.

(16) Matacotta, F. C.; Pal, D.; Mertelj, T.; Stastny, P.; Nozar, P.; Mateev, D.; Ganguly, P. *Solid State Commun.* **1992**, *84*, 781.

(17) Izumi, F.; Kinoshita, K.; Matsui, Y.; Yanagisawa, K.; Ishigaki, T.; Kamiyama, T.; Yamada, T.; Asano, H. *Physica C* **1992**, *196*, 227.

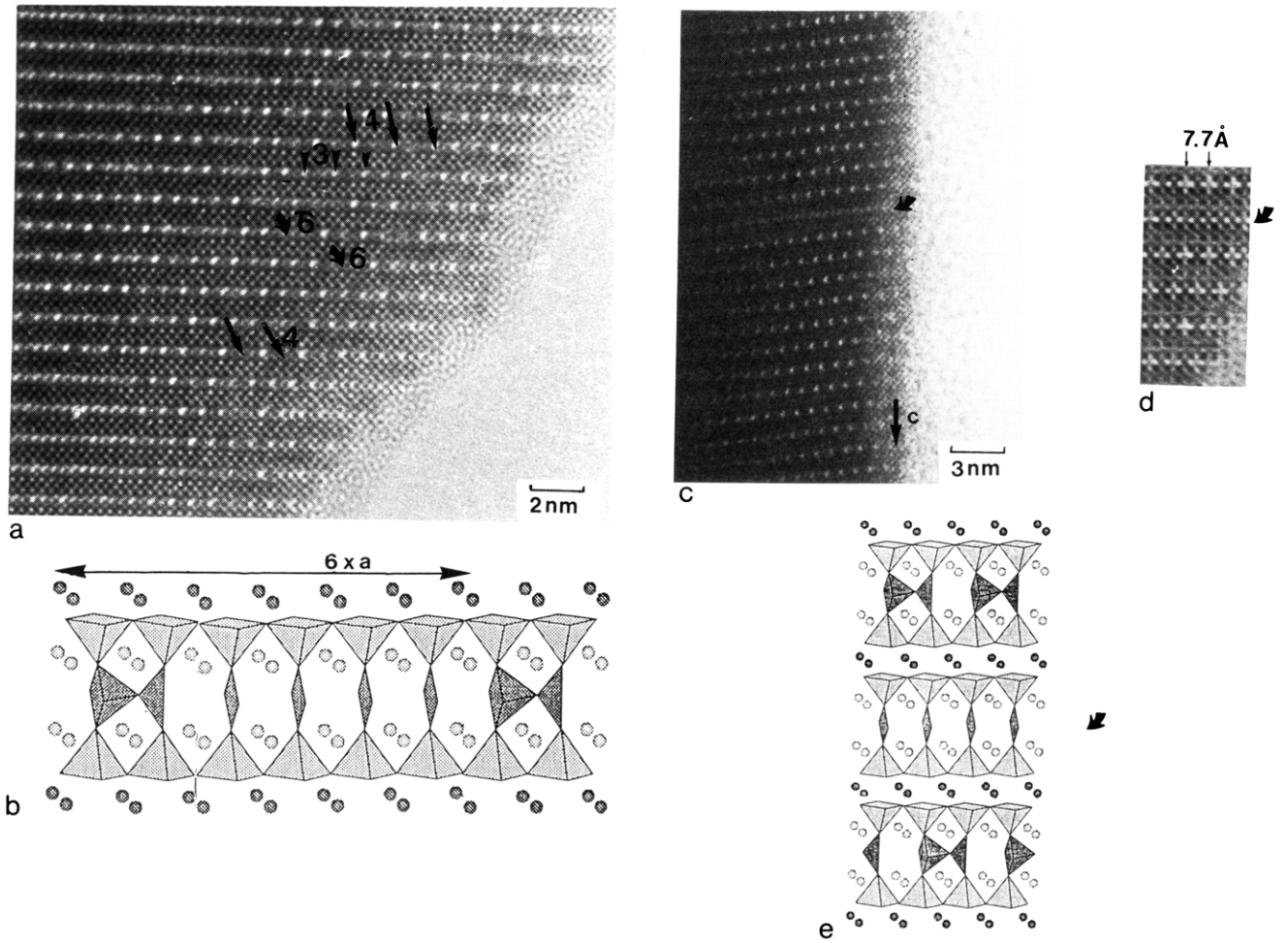

Figure 6. Intergrowth of members with $n \neq 2$: (a) experimental image where $n = 3$, 4, and 6 defects are observed. (b) Schematical drawing of the member $n = 6$ as example. A single row of copper atoms is sometimes observed: (c) $\Delta f \sim 20$ nm and (d) $\Delta f \sim -10$ nm. The schematical drawing is shown in (e).

dots correlated to the NO_3 and CO_3 groups. It can be seen that for a large part of the crystal, the spacing of these dots is of 7.7 Å, characteristic of the $n = 2$ matrix, but that from place to place this spacing has different values, of 11.55, or 15.4, or 23.1 Å, corresponding to a variation of the superstructure along $\vec{a}$, i.e., a equal to $3a_{123}$, $4a_{123}$, and $6a_{123}$ respectively. Such defects are easily interpreted as the members $n = 3$, 4, and 6 respectively; then their structure (Figure 6b) is described as the ordered stacking along $\vec{a}$ of rows of CuO_5 pyramids with rows of $CO_3(NO_3)$ groups and rows of CuO_4 square planar groups according to the sequence "$1CuO_5$–$1CO_3$–$(n-2)CuO_4$". In the same way, Figure 6c shows a single row of gray dots ($\Delta f \sim 20$ nm) (arrowed), which corresponds to one row of unsubstituted copper atoms, the same image for a focus value of $\sim$–10 nm is enlarged in Figure 6d. This defect corresponds to a pure "123" cuprate layer in the "123"-type oxycarbonitrate matrix (Figure 6e).

(2) *Oriented Domains.* The formation of 90° oriented domains is a frequent feature in these mixed materials; a similar behavior was reported for the pure carbonates $(Y_{1-x}Ca_x)Ba_4Cu_5CO_3O_{11}$.[10] Through these domains, the $\vec{c}$ axes are perpendicular and characteristic ED patterns (Figure 7a) are observed.

The size of the domains varies in a large range as shown in Figure 7b,c. In Figure 7b, one observes two large domains, [001] and [100], several ten thousands of nanometers wide. The boundary between these domains is not parallel to a peculiar plane and, in that case, is associated with a disturbed zone. In Figure 7c, the domains are considerably smaller, some nanometers wide. In that example, the zone axis is [010] for the two domains and the boundaries are parallel to (001) which is the common plane. In this image recorded for a focus value close to –60 nm, the contrast consists of two groups of staggered rows of white dots; the three rows of small dots are correlated to the positions of the (Y, Ca) and Cu(2) atoms of the pyramidal layer; the two rows of bright dots of the second groups are correlated to the barium positions. On the image 7c, it appears clearly that the Cu(2)–(Y,Ca)–Cu(2) triple layers ensure the connection between the two 90° oriented matrices and run at the boundaries. An idealized model can thus be proposed on Figure 7d. This model is similar to that previously proposed in the 123-type pure cuprates of the systems Ln–Ba–Cu–O, to explain similar features sometimes observed when the ordering between Ba and Ln is disturbed (T3 phase (11) or La/Ba $\sim$ 1[12,13]).

The formation of such boundaries takes its origin in two factors. The first deals with the fact the subcell of this structure is characterized by $a = b$, and c/b very close to 3, contrary to the classical 92 K superconductor, $YBa_2Cu_3O_7$; such a characteristic allows the ordering of the atoms along the three equivalent directions of the perovskite subcell. The second factor deals with the presence of calcium which can partly occupy the two types of cationic sites, yttrium and barium, and can also exhibit a different coordination; such a property is undoubtedly a favorable

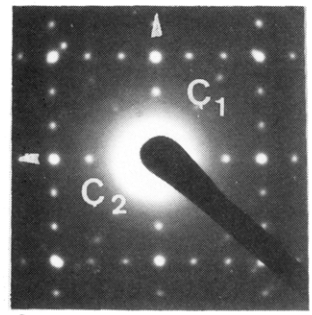

a

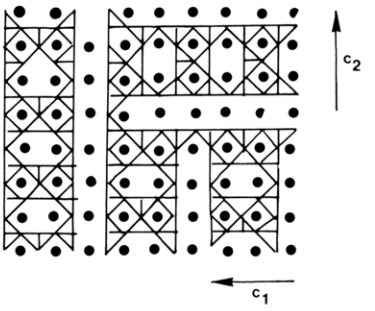

d

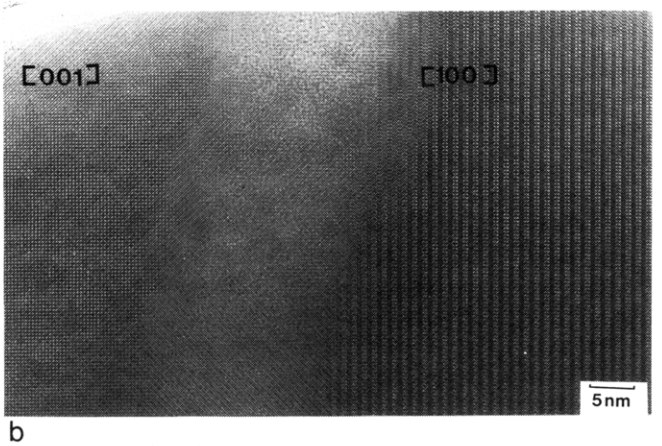

b

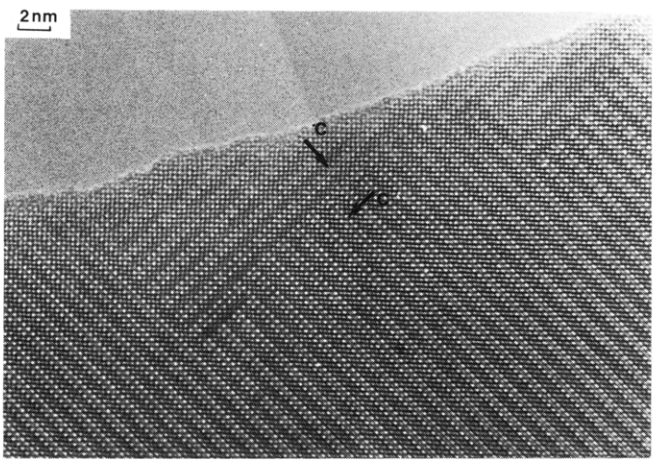

c

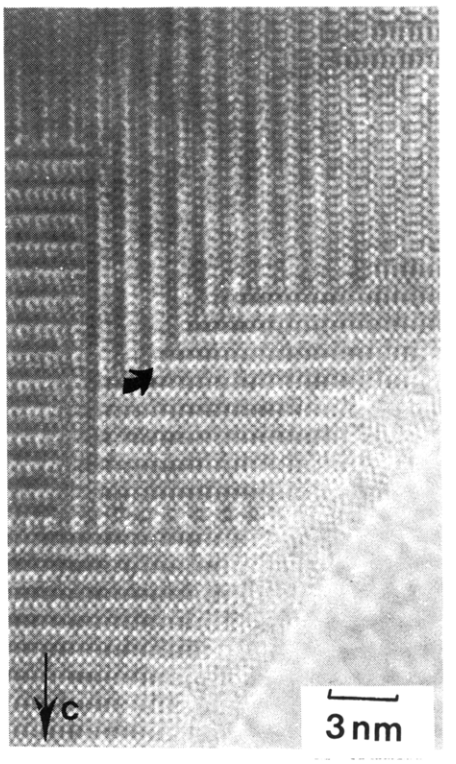

e

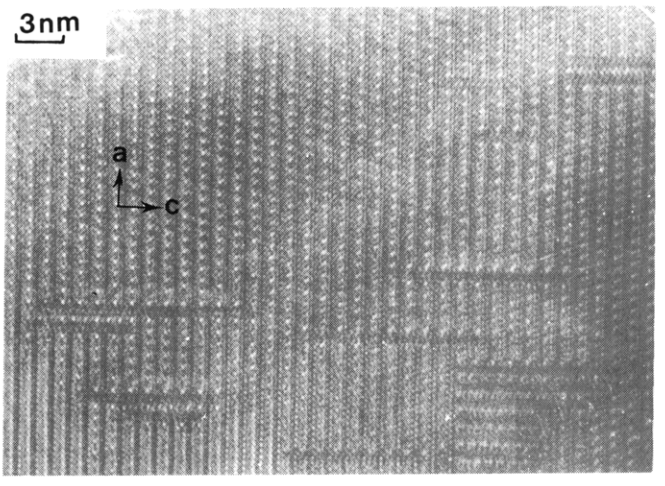

f

Figure 7. (a) Typical E.D pattern of two 90° oriented domains. (b) Example of large [001] and [100] domains. (c) Example of small [010] domain. The boundary is parallel to (001). (d) Idealized drawing of the (001) boundary. (e) Image of a (103) boundary. (f) Image of short 90° oriented segments.

parameter since it can be seen that the coordination of the A cation at the intersection of the boundaries is modified (10 instead of 9).

An important point related to these informations deals with the absence of twinning contrary to $YBa_2Cu_3O_7$. This observation is in agreement with the symmetry of the subcell which tends to be tetragonal. It may be due to the unability of the CO_3 (or NO_3) groups to be located in the twinning boundaries owing to their particular triangular geometry.

The easy change in orientation of the copper polyhedra, carbonate and nitrate groups, is also illustrated by two features shows in Figure 7e,f. The first one corresponds to the existence of domains whose boundaries are roughly parallel to (103), i.e., to the (110)p of the perovskite subcell. Such an orientation of the boundary can be easily described

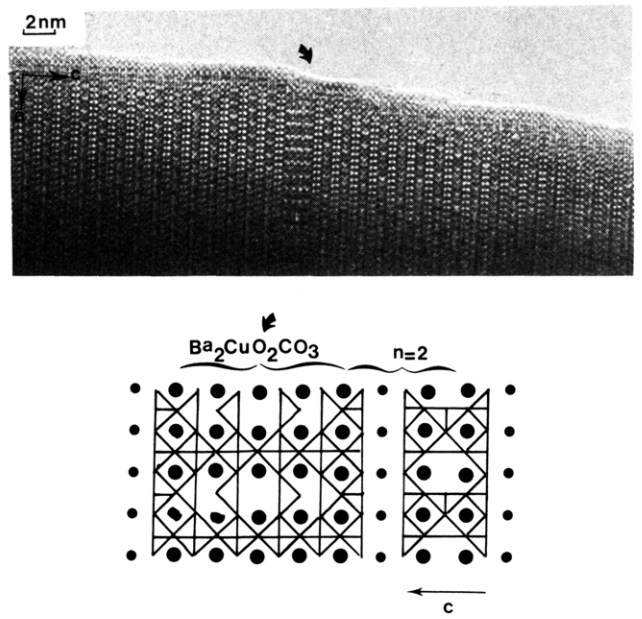

Figure 8. (a) Existence of four adjacent ($Ba_2CuO_2CO_3$) layers intergrown along the $\vec{c}$ axis with the oxynitrocarbonate $n = 2$ [010] image. (b) Idealized model of the defect.

from the regular transition of the layers connection described in model 7d. The second feature deals with the existence of isolated 90° oriented segments, some units wide, which take place in an aleatory way in the matrix (Figure 7f).

(3) Intergrowth of the "123" Oxycarbonate with the $Sr_2CuO_2CO_3$-Type Structure. Original defects corresponding to a variation of the stacking of the layers are observed. A first example is shown in Figure 8a for a [010] orientation. The white dots image the carbon and nitrogen atoms; the group of the three adjacent rows with the sequence of contrast [bright–gray–bright] are correlated to the $[CuO_2]_\infty$ layers and the intermediate (Y,Ca) layer. At the level of the defect (arrowed), these groups of three rows have disappeared and we observe four adjacent slices built up from one $[BaO]_\infty$ layer and one mixed carbon (or nitrogen)–copper layer; in these slices the periodicity "$2a$ = 7.7 Å" is kept on so that one C (or N) and one Cu atom alternate along $\vec{a}$.

This contrast is in fact similar to that encountered in the $Sr_2CuO_2CO_3$-type structure. Thus, a structural model can be proposed (Figure 8b). This defect can be described as a $Sr_2CuO_2CO_3$-type layer,[14-17] which is four octahedra wide along $\vec{c}$ and is connected in the (001) plane to a layer of corner-sharing CuO_5 pyramids, so that both structures, the "123" oxycarbonate $(Y_{1-x}Ca_x)_2Ba_4Cu_5CO_3O_{11}$ and the $Ba_2CuO_2CO_3$ structure, form a new intergrowth. Consequently, the composition of this defect can be formulated $(Y_{1-x}Ca_x)_2Ba_2Cu_4(Ba_2CuCO_3)_4O_{17}$. In other words, a new structural family with the generic formulation $(Y_{1-x}Ca_x)_2Ba_2Cu_4O_9(Ba_2CuO_2CO_3)_n$, characterized by various thicknesses of the octahedral layer n, is expected, $n = 4$ corresponding to the present defect and $n = \infty$ being represented by the hypothetical $Ba_2CuO_2CO_3$, which would exhibits a $(Sr_{2-x}Ba_x)CuO_2CO_3$ structure (Figure 9).[14-17] It should be possible to stabilize such phases by replacing partly barium by strontium. From this study it is also possible to predict the existence of intergrowths between the "123" type oxycarbonates and the $SrCuO_2CO_3$-type structure.

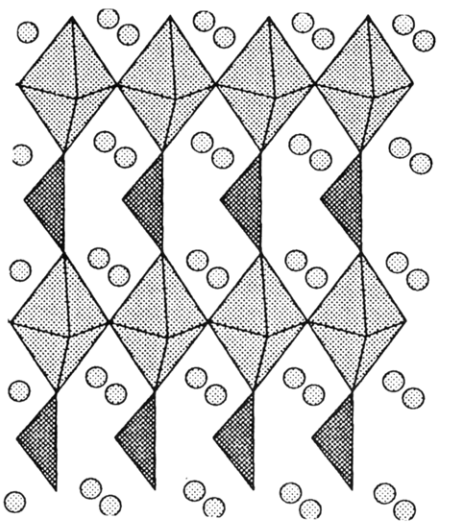

Figure 9. $(Sr_{2-x}Ba_x)CuO_2CO_3$ structure.

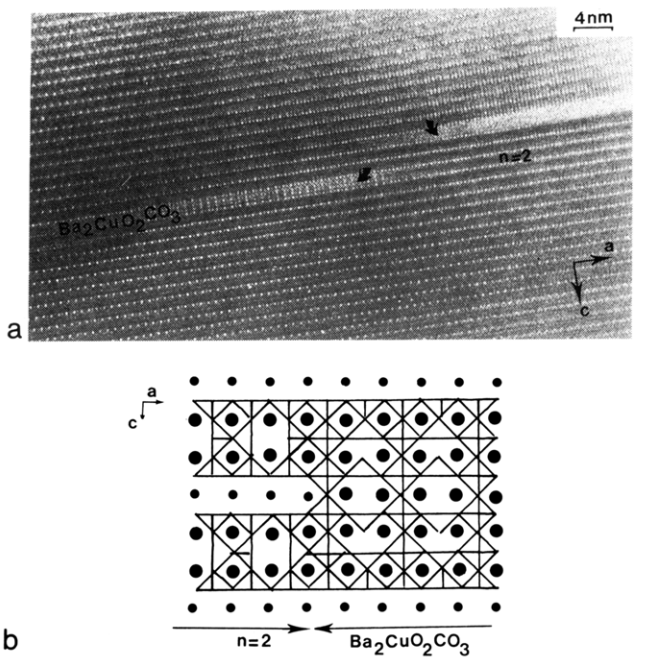

Figure 10. (a) [010] image of an intergrowth of the same species along the $\vec{a}$ axis. (b) Idealized model.

A second type of defect, which shows the ability of the "123"-type oxycarbonate and the "$Sr_2CuO_2CO_3$" structures to form intergrowths is shown in Figure 10a. On the right part of the slice (labeled $n = 2$) one recognizes the contrast characteristic of the "123" type oxycarbonitrate $(Y_{1-x}Ca_x)_2Ba_4Cu_5(C,N)O_{14}$, whereas on the left part (labeled $Ba_2CuO_2CO_3$) one obtains a different contrast characteristic of the "$Sr_2CuO_2CO_3$"-type structure. In that case, the two structures are no more connected along the (001) plane but along the (100) plane of the "123" structure. The corresponding structural model (Figure 10b) shows the easy lateral connection between the two structures: the boundary between the two structures consists of corner-sharing octahedra only.

Concluding Remarks

This study shows the ability of the perovskite framework to accomodate as well CO_3 as NO_3 groups without any formation of microtwinning contrary to the classical $YBa_2Cu_3O_7$ cuprate. It confirms the existence of 90° oriented

domains previously observed for the pure "123" oxycarbonates.[10] The existence of extended defects, characterized by a local variation of the spacing of the rows of CO_3 (or NO_3) groups demonstrates the high potential of this system for the generation of new members of the series $(Y_{1-x}Ca_x)_nBa_{2n}Cu_{3n-1}(C,N)O_3O_{7n-3}$. The most important feature deals with the discovery of a new type of defects involving intergrowths between the "123" type oxycarbonitrate and the $Sr_2CuO_2CO_3$-type structures. The latters suggest the possibility to synthesize new oxycarbonates and nitrates with the generic formulation $(Ln_{1-x}Ca_x)_2A_2Cu_4O_9(A_2CuO_2CO_3)_n$ with A = Ba, Sr, which might be superconductive. A systematic investigation of this system is in progress.